CHECIR, Volume *1*

Supplemental information

Molecule-to-molecule conversion of RCF lignin oil to sustainable aviation fuel

Bruno Pandalone, Senne Delanghe, Deepak Raikwar, Francesco Brandi, Thuan A. Vo, Yingtuan Zhang, and Bert F. Sels

Electronic Supporting Information (ESI)

Unlocking Lignin Oil's Potential: Molecule-to-Molecule Pathways in Sustainable Aviation Fuel (SAF) Production from Lignin

*Bruno Pandalone[a], Senne Delanghe[a], Deepak Raikwar[a], Francesco Brandi[ab], Thuan A. Vo[a], Yingtuan Zhang[a], Bert F. Sels[a]**

[a]Center for Sustainable Catalysis and Engineering (CSCE), KU Leuven, Celestijnenlaan 200F, 3001 Heverlee, Belgium

[b]National Research Counsil-Institute of Chemistry of Organometallic Compounds (CNR-ICCOM), Via Madonna del Piano 10, Sesto Fiorentino 50019, Italy

** Corresponding author*

Tel: +32 16321610

Email: bert.sels@kuleuven.be

A. EXPERIMENTAL

1. Chemical and materials

All commercial chemicals were analytic reagents and were used without further purifications. 5 wt% Ru/C (product reference: 206180), tetrahydrofuran (>99%, stabilized with 250 ppm BHT), DMSO-d6 (99.9 % atom D), N-methyl-N-(trimethylsilyl)trifluoroacetamide (>98.5%), 2-isopropylphenol (>98%) and anhydrous pyridine (99.8%) were purchased from Sigma Aldrich. Dodecane (99.9%) was purchased from TermoFisher Scientific. Phenanthrene (99.0%) was purchased by TCI Europe. Ethyl acetate (99.5%), n-heptane (>99%), ethanol (99.9%), methanol (99.9%) were purchased from Acros Organics. Pine was obtained from a local dealer (Aveve), milled to obtain a sawdust fraction.

2. Reductive Catalytic Fractionation (RCF)

The RCF experiment was performed in a 2 L stainless steel batch reactor (Parr Instruments & Co.). 150 g of pine wood was loaded into the reactor, together with 15.0 g of Ru/C catalyst and 800 mL methanol. Subsequently, the reactor was sealed, flushed three times with N_2 (10 bar), and pressurized with H_2 (30 bar at room temperature). Next, the reaction mixture was stirred (750 rpm) and simultaneously heated to 235 °C (≈30 min heating time). After the reaction time of 3 h, the reactor was cooled and depressurized at room temperature. The reactor contents were quantitatively collected by washing the reactor with acetone. The solid pulp was separated by filtration and washed thoroughly with acetone. Next, the resulting filtrate was evaporated, and a brown oil was obtained, which was subjected to a threefold liquid-liquid extraction using Ethyl Acetate (EtOAc) and water. The EtOAc-extracted phase was then separated from the water phase and dried at 80 °C overnight to finally collect the refined lignin-oil (RLO). The reaction was performed twice and around 30 g of RLO were produced which were employed for the solvent-based fractionation step.

3. Fractionation of lignin oil

The fractionation of RCF lignin oil was executed following the procedure described by Van Aelst et al.[1] Totally, 30 g of lignin oil was threefold extracted at 80 °C for 0.5 h, with heptane and ethyl acetate (EtOAc) as solvent. The fractionation began with 100% heptane, and the solvent polarity was gradually increased by raising the volume of EtOAc by 20% each step. At each stage, the RLO was separated into a liquid (soluble) fraction, which was collected, and a solid (insoluble) fraction, which was used as

starting material for the next step. The soluble and insoluble fraction were dried by rotary evaporation to determine their weight prior to starting each next step. Approximately, the amount of solvent was in ml 5x times the weight in grams of the solid fraction used.

In total 30g of RLO were divided into six distinct liquid fractions: H100 (100% heptane), H80 (80% heptane/20% EtOAc), H60 (60% heptane/40% EtOAc), H40 (40%heptane/60% EtOAc), H20 (20% heptane/80% EtOAc) and E100 (100% EtOAc). The individual mass of the fractions, and their weight percentage (wt%) relative to the initial RLO mass were as follow: H100 yielded 12 g (40 wt%), H80 yielded 3.2 g (10.7 wt%), H60 yielded 5.2 g (17.3 wt%), H40 yielded 4.5 g (15 wt%), H20 yielded 2.4 g (8 wt%), and E100 yielded 1.3 g (4.3 wt%). The mass and corresponding weight percentages of each fraction are summarized in **Table S1**. A schematic representation of the fractionation is shown in **Scheme S1**, and the relative distribution of the fractions is illustrated in **Figure S1**.

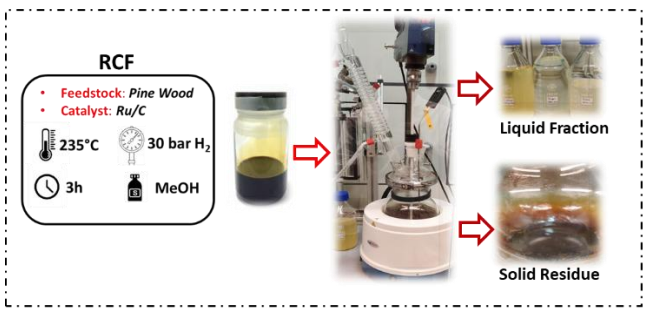

Pine Ru/C RLO	30 g
H100	12 g
H80	3,2 g
H60	5,2 g
H40	4,5 g
H20	2,4 g
E100	1,3 g
Residue	0,49 g
TOTAL	29 g

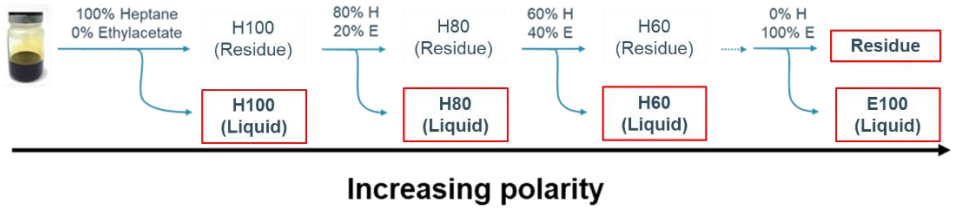

Scheme S1. Schematic representation of RLO fractionation according to the described procedure.

Table S1. Mass yield of the obtained fraction (H100-E100), relative weight compared to the original feedstock (RLO), and molar mass distribution.

	H100	H80	H60	H40	H20	E100	Residue	RLO
Weight of fraction (g)	12.0	3.2	5.2	4.5	2.4	1.3	0.5	30.0
Relative weight (wt %)	40.0	10.7	17.3	15.0	8.0	4.3	1.6	//
Mw (g mol^{-1})	157	280	418	604	932	1430	2728	612
Mn (g mol^{-1})	126	229	328	492	772	1108	1384	329
D (Mw/Mn)	1.25	1.22	1.27	1.23	1.20	1.29	1.97	1.86

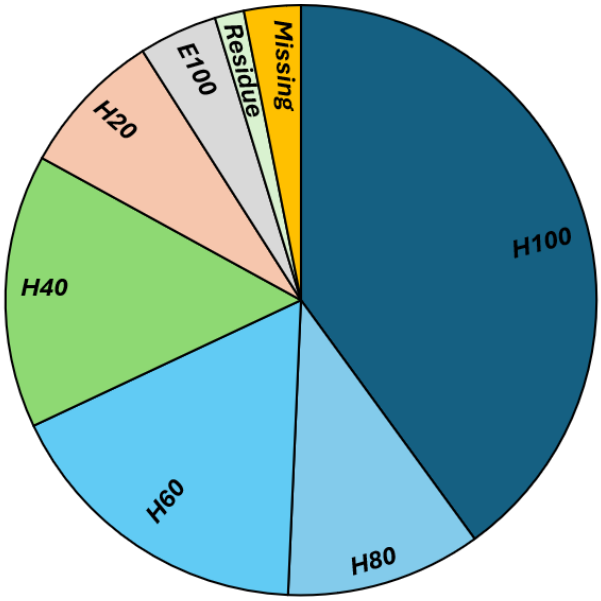

Figure S1. Weight distribution of the obtained fraction (H100-E100)

4. Hydrodeoxygenation (HDO) of lignin oil

The HDO experiment was performed in a 50 mL stainless steel batch reactor (Parr Instruments & Co.). 500 mg of feedstock (lignin oil and fractions) was loaded into the reactor, together with 400 mg of catalyst (Ni_2P/SiO_2) and 20 mL dodecane. Subsequently, the reactor was sealed, flushed three times with N_2 (6 bar) and one time with hydrogen (10 bar) then pressurized with H_2 (50 bar at room temperature). Next, the reaction mixture was stirred (700 rpm) and simultaneously heated to 300 °C (~45 min. heating time). After the reaction time of 5h, the reactor was cooled and depressurized at room temperature. The reactor contents (liquid phase and solid catalyst) were quantitatively collected with a glass pipette. The solid catalyst was separated by centrifugation and washed three times with heptane to remove any solid residues. The catalyst was then dried overnight at 100 °C, making it ready for re-reduction and subsequent reuse in either analytical evaluation or additional HDO experiments. The liquid fraction was collected in a separate vial and directly injected into GC-MS/FID for identification and quantification of hydrocarbons without further treatment.

5. GPC analysis of lignin oil and fractions

The distribution of the molar mass of the lignin products was investigated using gel permeation chromatography – size exclusion (GPC-SEC). Therefore, a lignin sample was solubilized in THF (5 mg mL^{-1}) and subsequently filtered with a 0.2 µm polytetrafluoroethylene (PTFE) membrane to remove any PM to prevent plugging of the column. GPC-SEC analyses were performed at 40 °C on a Waters E2695 equipped with a PL – Gel 3 µm Mixed-E column with at length of 300 mm, using THF as a solvent with a flow of 1 mL min^{-1}. The detection was ultraviolet (UV) based at a wavelength of 280 nm. Calibration were based on calibration with commercial polystyrene standards of Agilent (with Mw ranging from 166 g mol^{-1} to 27810 g mol^{-1}. Based on these standards the weight average molecular weight (Mw) and the number average molecular weight (Mn) can be calculated utilizing the following formula with Mi the molecular weight of a molecule n, Ni the number of molecules with that molecular weight and c_i the concentration of a molecule i.

$$\textbf{Number average molecular weight} = \overline{Mn} = \frac{\sum c_i}{\sum \frac{c_i}{M_i}} = \frac{\sum N_i M_i}{\sum N_i} \quad (1)$$

$$\textbf{Weight average molecular weight} = \overline{Mw} = \frac{\sum c_i M_i}{\sum c_i} = \frac{\sum N_i M_i^2}{\sum N_i M_i} \quad (2)$$

$$\textbf{Polydispersity} = D = \frac{\overline{Mw}}{\overline{Mn}} \quad (3)$$

6. ^{1}H - ^{13}C 2D HSQC NMR and ^{31}P NMR Analysis of lignin oil and fractions

^{1}H-^{13}C 2D HSQC NMR

The two-dimensional ^{1}H - ^{13}C HSQC NMR analysis was executed following the standardized procedure in our lab in accordance with Van Aelst et al.[1] Approximately 70 mg of the lignin sample was dissolved in 0.6 mL DMSO-d6 and loaded in an NMR tube. The two-dimensional ^{1}H - ^{13}C HSQC NMR experiment was conducted at 25 °C using a Bruker Avance III HD 400 MHz console with a Bruker AscendTM 400 Magnet, equipped with a 5 mm PABBO probe. A Bruker standard pulse sequence ('hsqcetgpsp.3') was used for semi-quantification with the following parameters: spectral width in F2 dimension (^{1}H) of 13 ppm using 2048 data points, a spectral width in F1 dimension (^{13}C) of 165 ppm, using 256 data points, a total of 16 scans were recorded with a 2s interscan delay (D1). The Bruker standard pulse sequence (hsqcedetgp') was used for qualification with the following parameters: spectral width in F2 dimension (^{1}H) of 13 ppm using 1024 data points, a spectral width in F1 dimension (^{13}C) of 165 ppm using 256 data points. Depending on the sample, the amount of scans varied between 2 and 16. Bruker's Topspin 4.0.2 software was used for data processing and volume integration. The spectra were processed in 2048 data points in the F2 and F1 dimensions (with one level of linear prediction and 32 coefficients). The solvent peak of DMSO was used as the internal reference (δC/δH: 39.5 ppm/2.49 ppm) following by manually phasing and automatic baseline correction.

^{31}P-NMR analysis

^{31}P-NMR measurements were performed to obtain the OH content of lignin samples using a standard phosphitylation procedure. A solvent mixture (1.6 pyridine: 1 CDCl3) was used to prepare stock solutions of the internal standard (cholesterol, 20 mg/mL) and relaxation agent (chromium acetylacetonate, 10 mg/mL). Approximately 20 mg of lignin was weighed, and 100 µL of the internal standard solution, 50 µL of the relaxation agent solution, and 400 µL of the solvent solution were added. After adding 75 µL of 2-chloro-4,4,5,5-tetramethyl-1,3,2-dioxaphospholane (TMDP), the sample was thoroughly mixed and transferred to an NMR tube. 31P-NMR spectra were acquired on a Bruker Avance III 400 MHz NMR using a standard phosphorus pulse sequence (128 scans, 6 s interscan delay, O1P 140 ppm). Chemical shifts were calibrated to the sharp water + TMDP peak at 132.2 ppm, with automatic baseline correction applied.

7. Two-dimensional gas chromatography (GCxGC) for lignin oil and fractions

The phenolic monomers and dimers of the oil and its derived fractions were quantitatively analyzed by GCxGC. Therefore, a weighed amount of external standard (2-isopropyl phenol; 30 mg) was added to a GC-vial containing a weighed amount of sample (100 mg). Subsequently, this mixture was dissolved in 1 mL of Tetrahydrofuran (THF). From this mixture, 0.1 mL was taken and mixed in a small GC vial with 0.07 mL of N-methyl-N- (trimethylsilyl)trifluoroacetamide and 0.65 mL of Pyridine. The vial was sealed and put in an oven at 80 °C for 30 min. Afterward, the samples were analyzed on a

GCxGC (Shimadzu 2030). The GCxGC comprises a BPX5 column (20 m × 0.18 mm × 0.18 µm) as the first-dimension column connected to a BPX50 (5 m × 0.25 mm × 0.1 µm) as the second-dimension column. The column set and a flow modulator (SepSolve) are placed in the same oven. The outlet of the second column is connected to an FID/MS detector. For the GCxGC-FID setup, the flow rates of H_2, air, and N_2 (make-up gas) were set at 35, 350, and 35 mL min^{-1}, respectively. The FID temperature was set at 350 °C and the data acquisition rate was 100 Hz. Moreover, a PTV injector was used in these analyses with a programmed temperature injector from 40 °C to 340 °C (hold 25 minutes at 340 °C) to avoid discrimination in the injector. For the GCxGC-MS setup, the scanning range was set from 50 to 700 m/z. The GC-MS interface (transfer line) temperature was set at 350 °C and the ion source temperature was set at 280 °C. The modulation period was set at 4 s to obtain a maximal resolution in the first dimension without causing wrap-around. The GC system was operated in programmed temperature conditions: 50 °C to 350 °C with a heating rate of 4 °C min^{-1}.

Monomers Identification

In total, 18 different monomers were identified across the derived fractions, see **Scheme S3**. The monomers were identified by injecting the standard or, where standard was not available via comparing deconvoluted mass spectra from GCxGC-MS with the NIST library. Additionally, comparison with previous work by Dao Hang and Van Aelst et al. helped in validating the results from GCxGC and expanding the number of identified monomeric structures.[2]

Dimers Identification

In addition to the 18 identified monomers, 46 different dimers were identified distributed over the various fractions and the entire RFLO, see **Tables S3-S11**. However, the identification of those dimers presented challenges. Unlike the monomers, it was not possible to rely on deconvoluted mass spectra compared to the NIST library or purchased pure dimers. Consequently, the identification of dimers was accomplished through a detailed analysis of their mass fragmentation spectra. To confirm the accuracy of these identifications, we referred to the study by Dao Hang and Van Aelst et al. for validation.[2] Moreover, due to the lack of purchasable authentic dimers, we were unable to obtain calibration curves and response factors (RFs) for the individual dimers. Nevertheless, RFs evaluation was carried out by referencing the effective carbon number (ECN) of identified molecules relative to an external standard, isopropyl phenol.[3] The RFs were calculated under the assumption that the response factor for each molecule on the FID detector is related to the number of carbon atoms, functional groups, and the number of oxygen atoms present in the form of methoxy groups and phenolic OH.[3]

Monomers and Dimers Quantification

The amounts of different compounds were calculated as follows:

$$Yield\ (x)[\%] = \frac{\frac{A_X}{A_{IS}} * \frac{mmol_{IS}}{RF_X} * M_X}{lignin\ oil\ (mg)} * 100$$

$$Total\ Yield\ [\%] = \sum_{X=0}^{n} Yield\ (x)$$

With A representing the area, RF the response factor based on calibration curves or ECN, and M the molar mass. The X refers to a generic molecule in the mixture, while IS to the internal standard. The amount of lignin oil considered is the oil injected into GC.

Quantification of Unidentified Monomers and Dimers

Along with most identified monomers and dimers, a fraction of unidentified compounds was included in the quantification to determine a more complete mass balance for all the fractions. Given the low concentration present in the products, it was not possible for some peaks to perform an accurate identification. In this case, these compounds were categorized as unknown. However, it was possible to rely on the retention time, compared to the identified compounds in order to categorize these compounds as unknown monomers or dimers. As a result of this investigation, the unknown compounds were divided as follows:

Category	Retention time (min)
Monomers	5 - 21
Dimers	21 - 50

The quantification of the unidentified compounds was achieved with the same methodology for the identified compounds as explained earlier. However, in this case A, RF and M were defined differently. First, the area is defined as the difference between the cumulative area calculated through integration of the full chromatogram in a specific region defined by a range of retention time listed above, and the cumulative area of identified compounds in that region. Therefore, the RF and the M are both defined as the average number of RF and M of identified compounds present in a region defined by the retention time as listed above. With the present procedure it was possible to define a precise estimation of the yield for monomers and dimers that were not possible to identify due to the low concentration in the products.

8. One-dimensional GC-MS/FID for HDO products

The quantitative and qualitative analysis of the HDO products composition was performed using GC-FID/MS system GCMS-QP2010 SE (single quadrupole) equipped with an AOC-20i Plus auto – injector. The injection volume was 1 µL with a split ratio of 1:20 into a 350 °C injection temperature. The GC was equipped with a 30 m SH-I-5HT column with an internal diameter of 0.25 mm and a film thickness of 0.25 µm. Following temperature program was used in the oven: 1 minute at 40 °C, heat up to 380 °C (heat rate 10 °C/min) and this temperature was kept constant for 5 min. He (150 kPa, total flow = 61.2 mL/min) served as a carrier gas. After elution, the eluate was split to both detectors using a passive Silflow 4-port splitter with an FID/MS split ratio of 1/0.15. The MS detector uses a 200 °C ion source and was used to identify peaks in the chromatogram. This detector was used as a qualitative assessment whereas the FID detector was used as a quantitative assessment. Prior to the analysis, the samples were prepared by mixing 1 mL of HDO products with 50 µL of a prepared internal standard solution (IS). The IS consists of 0.504 g of phenanthrene (internal standard) in 10 g of dodecane (solvent).

8.1 Identification of hydrocarbons in the liquid products from HDO

All the liquid products were analyzed for identification of the hydrocarbons with GC-MS as described earlier in Section 8. The identification of the majority of hydrocarbons present in the liquid products was executed by comparing the deconvoluted mass spectra with the NIST library that was mostly reliable for hydrocarbons in the C6 to C11 range. In general, for the hydrocarbons ranging from C12 to C18 it was not possible to rely on the NIST library. In this case, the structures of the hydrocarbons were assigned based on the information on the lignin-derived molecules (mostly dimers) present in the different fractions. Herein, it was possible to predict the structure of the hydrocarbons after HDO, which were further confirmed by investigating the fragmentation spectra from MS analysis.

8.2 Quantification of identified hydrocarbons in the liquid products from HDO

The quantification of the identified hydrocarbons in the liquid products was executed with one-dimensional GC equipped with FID detector as explained earlier in this section. The yield of the identified hydrocarbons, for a generic compound X, is expressed as carbon yield relative to the theoretical maximum (relative carbon yield) calculated as shown below:

$$Relative\ carbon\ yield\ (\%) = \frac{molC_{product}(x)}{0.9 * molC_{feedstock}} * 100 \quad (3)$$

Therefore, the total relative carbon yield was determined as sum of the relative carbon yield evaluated for a generic compound X in the liquid products:

$$Total\ Relative\ carbon\ yield\ (\%) = \sum_{x=0}^{n} \left(\frac{molC_{product}(x)}{0.9 * molC_{feedstock}} * 100 \right) \quad (4)$$

The carbon mole in the products used in the eq. (3) were quantified as follows:

$$molC_{product}(x) = mol_{product}(x) * C_n \quad (5)$$

With C_n the carbon number of the identified compound X. While the mol of a generic compound X identified in the total liquid products were evaluated as follows:

$$mol_{product}(x) = \frac{A_X}{A_{IS}} * \left(\frac{mol_{IS}}{RF_X} \right) * fraction \quad (6)$$

With A representing the area from GC-FID, and RF the response factor based on the effective carbon number (eq.6)[3]. Due to the lack of purchasable authentic hydrocarbons, we were unable to obtain calibration curves and response factors (RFs) for the individual molecules. However, RFs evaluation was carried out by referencing the effective carbon number (ECN) of identified molecules relative to an external standard, phenantrene[3]. The RFs were calculated under the assumption that the response factor for each hydrocarbon on the FID detector is solely related to the number of carbon atoms.[3] In addition, in order to quantify the mol of products present in the entire liquid sample after HDO, a fraction (eq.6) was defined as the ratio between the mass of sample injected in the GC-FID and the total mass of liquid products.

Additionally, the moles of carbon present in the feedstock were evaluated based on the elemental analysis carried out for the six fractions and the RLO, as shown in the table below:

Elemental analysis							
	H100	**H80**	**H60**	**H40**	**H20**	**E100**	**RLO**
C (wt%)	68.4	64.8	64.9	64.4	63.3	64.4	67.6
H (wt%)	8.3	7.1	7.0	6.9	6.6	6.3	7.7
O (wt%)	20.4	25.5	26.0	26.2	26.4	25.6	24.2
$\boldsymbol{mmolC_{feedstock}}$*							
	H100	**H80**	**H60**	**H40**	**H20**	**E100**	**RLO**
mmol C in 1 g LO	56.0	54.0	54.0	53.6	52.7	53.6	56.2

The moles of C in the feedstocks*, were calculated based on the C (wt%) from elemental analysis as presented in the eq. below:

$$mmolC_{feedstock} = \frac{C(wt\%)}{12.011 * 100} \quad (7)$$

Therefore, the relative carbon yield is adjusted by a factor 0.9, considering the theoretical maximum, that considers the unavoidable carbon loss during the deoxygenation process, which generates gaseous products from the methoxy groups of lignin-derived phenolic units. The theoretical maximum obtainable from all the employed feedstocks through HDO was determined based on eq.8 below:

$$C_{10}H_{14}O_3 + 7H_2 \rightarrow C_9H_{18} + CH_4 + 3H_2O \quad (8)$$

The equations were derived by considering the conversion of the entire lignin-oil into propyl cyclohexane with methane and water as the only by-products. A similar approach was reported by Cao et al.[4] In this way, it was possible to assume that 90% of the carbon is retained in the hydrocarbons after HDO, while 10% is lost due to the formation of gaseous products as result of the deoxygenation on the methoxy groups in the structures.

The general formula for the lignin-oil was assumed as $C_{10}H_{14}O_3$, determined through different assumptions, combined with elemental analysis (Section A.9) and $^{1}H–^{13}C$ HSQC NMR (Section A.6). First, the β–O–4 unit (see below) was considered as representative for the entire feedstock.

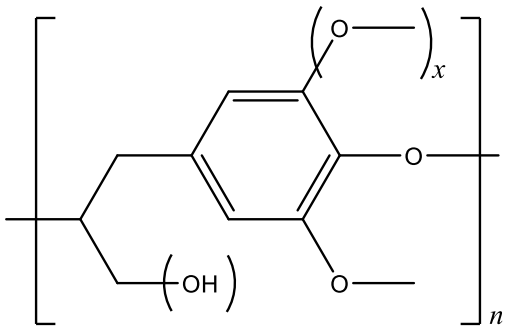

Therefore, its carbon number was adjusted according to its percentage of syringyl units (x in the β–O–4 unit above) calculated via $^{1}H–^{13}C$ HSQC NMR, as presented in the table below. Second, the content of hydrogen and oxygen was adjusted to their relative content to the carbon according to the elemental analysis.

$\boldsymbol{C_{10+x}H_yO_z}$	$\boldsymbol{x = syringyl\ content}$	$\boldsymbol{y = \frac{10+x}{mol\ C} * mol\ H}$	$\boldsymbol{z = \frac{10+x}{mol\ C} * mol\ O}$
RLO	0.012	13.64	2.69

Importantly, the quantification of every single hydrocarbon was carefully performed without taking into account any peak that represented a product coming from the solvent. The employed solvent for the reaction is dodecane and its presence in the reaction environment with the presence of active $Ni2P/SiO_2$ catalyst can lead to the formation of several linear components, such as undecane, decane, octane and heptane. To carefully avoid the presence of these products in the final analysis, a blank reaction was performed following the conditions reported in Section A.4 without the presence of lignin oil in the reactor. All the identified peaks after this blank reaction were carefully removed from

the analysis of the HDO products where lignin was employed as feedstock. A table including all the molecules identified in the chromatogram and considered as products from the solvent are listed below:

RT (min)	C_n	NAME	STRUCTURE
1.844	3	Propane	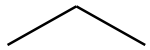
1.933	4	Butane	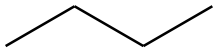
2.078	5	Iso-Pentane	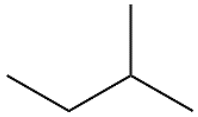
2.115	3	Acetone*	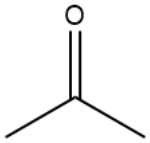
2.151	5	Pentane	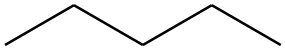
2.548	6	3-methylpentane	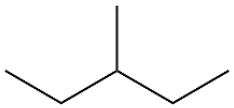
2.868	4	Tetrahydrofuran*	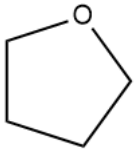
2.656	6	Hexane	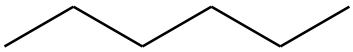
3.632	7	Heptane	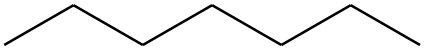
5.104	8	Octane	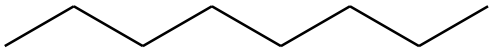
6.841	9	Nonane	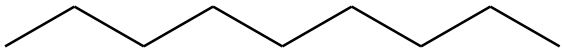
8.634	10	Decane	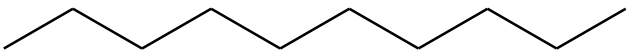
10.370	11	Undecane	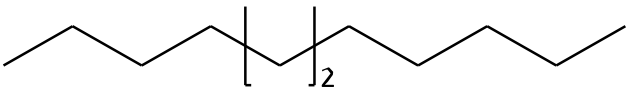
12.518	12	Dodecane	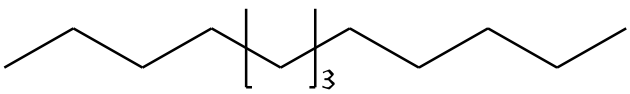
13.581	13	Tridecane	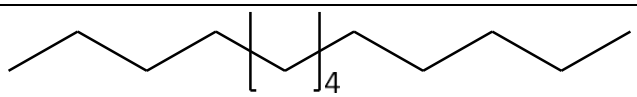
14.987	14	Tetradecane	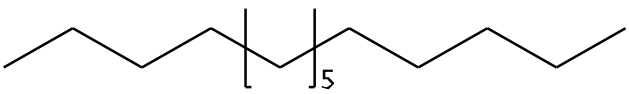

16.345	15	Pentadecane	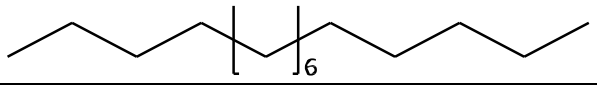
17.650	16	Hexadecane	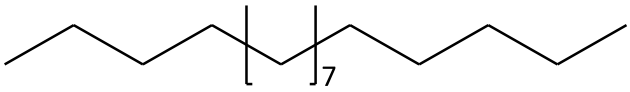
18.983	17	Heptadecane	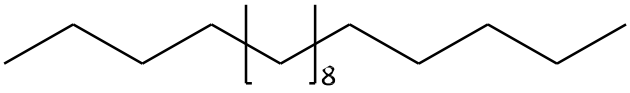
24.908	21	Heneicosane	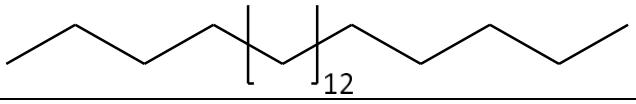

The listed* products are used to wash the reactor and the GC needle. For this reason they are found in small concentration in the products after GC analysis.

8.3 Quantification of unidentified hydrocarbons in the liquid products from HDO

Along with the majority of identified compounds present in the liquid products, a fraction of unidentified compounds was included in the quantification to determine the yield of liquid hydrocarbons after HDO of the different employed feedstocks. Given the low concentration present in the liquid products, it was not possible for some peaks to rely on comparison of the deconvoluted mass spectra with the NIST library. In this case, these compounds were categorized as unknown. However, it was possible to rely on the retention time, compared to the identified compounds in order to categorize these compounds based on the carbon number. As result of this investigation, the unknown compounds were divided as listed below:

Carbon Number	Retention time (min)
C < 8	0 - 6.5
C_9	6.5 - 8.2
$C_{10} – C_{13}$	8.2 - 15.1
$C_{14} – C_{15}$	15.1 - 17.8
$C_{16} – C_{18}$	17.8 - 22.9
$C_{19} – C_{27}$	22.9 - 49.9

In particular, due to the low concentration of hydrocarbons with C > 18, their identification was particularly challenging. However, those compounds made up a significant fraction of products derived from HDO of larger fractions such as H40 and H20 (See Section A.3). In this case, to have an estimated carbon number for all the products, the single peaks in the region 22.9 < RT < 49.9 were analyzed and based on the dominant mass in the MS spectra of those peaks, a carbon number was estimated considering the molecular formula of produced hydrocarbons as CH_2 with a mass of 14 g mol^{-1}.

The quantification of the unidentified compounds was achieved with the same methodology for the identified compounds as explained earlier in Section 8.2. However, in this case the A, the RF, and the Cn were determined differently. First, the area is defined as the difference between the cumulative area calculated through integration of the full chromatogram in a specific region defined by a range of retention time listed above, and the cumulative area of identified compounds and solvent related peaks in that particular region. Therefore, the RF and the Cn are both defined as the average number of RF and Cn of identified compounds present in a region defined by the retention time as listed above. With the present procedure it was possible to define a precise estimation of the relative carbon yield

for hydrocarbons that were not possible to identify due to the low concentration in the liquid products.

9. Elemental Analysis

The carbon, hydrogen, and oxygen content content for the six fractions and the RLO was measured using a Thermo Fisher Scientific FlashSmart Elemental Analyzer, equipped with a multivalve control (MVC) module. The analyzer includes a pre-packed argon-sealed quartz reactor which includes a pre-layer of 60mm of nickel-plated carbon prior to the quart chamber. The reactor is connected to an adsorption Pyrex filter, and the carrier gases, oxygen and helium, passes then through the GC column to the TCD detector. The GC column is made of stainless steel, with a length of 1 meter and a diameter of 6x5 mm. For the analysis, 1 to 5 mg of sample are used.

B. SUPPLEMENTAL NOTES

1. GPC Analysis

The GPC analysis, detailed in Section A.5 of the ESI, provided crucial insights into the size distribution of lignin-derived molecules across the six fractions. The key findings including weight (Mw) and number average (Mn) molecular weights, and the polydispersity (D) for both the fractions and the entire RLO are summarized in **Table S1**. The GPC chromatograms (**Figure S2a**) show how the lignin-derived molecules present in the original RLO are homogeneously distributed over the six fractions (H100-E100). Specifically, H100 is primarily composed of lignin-derived monomers, while the content of dimers increases from H100 to H60, with H60 exhibiting the highest concentration. Furthermore, H40 contains the highest concentration of trimers, while H20 and E100 are predominantly composed of larger oligomers (**Figure S2a**). This progression is attributed to the increasing polarity of the extractive solvent, which enhances the solubility of larger lignin fragments, as also described by Van Aelst et al.[92] The enrichment in high-molecular-weight molecules from H100 to E100 is further supported by the Mw and Mn listed in **Table S1**. These values steadily increase from 157 g mol^{-1} (H100) to 1430 g mol^{-1} (E100), and from 126 g mol^{-1} (H100) to 1108 g mol^{-1} (E100), respectively. In addition, the six fractions show a lower polydispersity (D=1.20-1.29)—highlighting a more homogenous molecular weight distribution—compared to the original RLO (D=1.86).

The GPC chromatograms in **Figure S2a** indicates that the extraction selectivity for different types of monomers shifts as the polarity of the extractive solvent changes. In particular, H100 shows a large peak around 166 g mol^{-1}—characteristic of propyl-guaiacol—while H80 and H60 show a peak around 182 g mol^{-1}—characteristic of propanol-guaiacol. By progressing with the polarity from H100 to E100, the peaks shift progressively toward higher Mw. The wide peaks at around 200-300 g mol^{-1}, 300-400 g mol^{-1} are attributed to dimers and trimers, respectively. In contrast with monomers, the wide big peak of dimers and trimers comprise multiple molecules and cannot be straightforwardly assigned to a single species. Nevertheless, the cumulative GPC chromatograms of all the fractions, normalized by their weight percentages relative to the original RLO, was found similar to the chromatogram of the entire RLO (**Figure S2b**), assessing the reliability of the analysis.

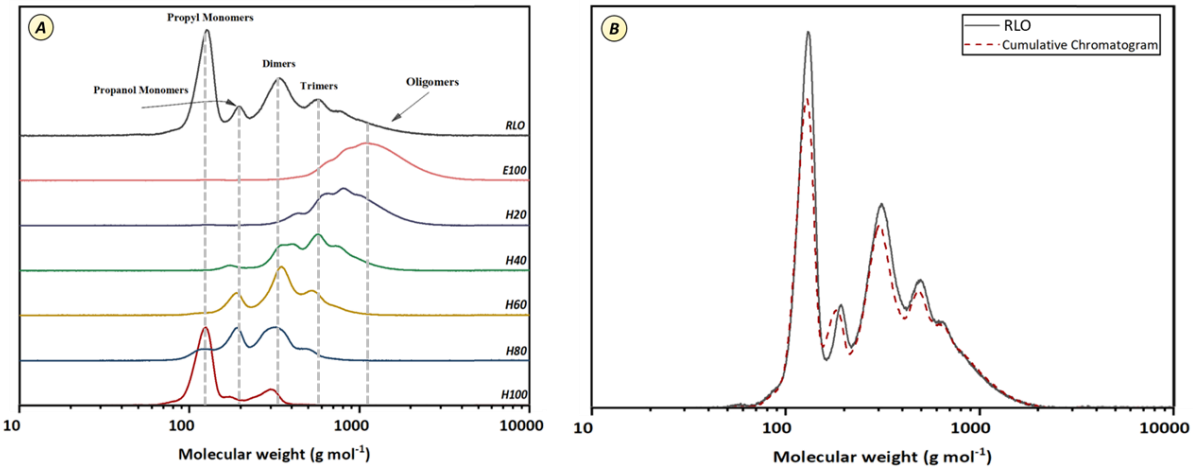

Figure S2. a) Molecular weight distribution from GPC for the obtained fractions (H100-E100) and the original RLO and **b)** Cumulative weight distribution of different fractions normalized by the weigh relative percentage compared to the original feedstock.

Nevertheless, the solvent-based fractionation generates a solid residual fraction (Residue) that is insoluble in all the solvents used for the fractionation. This residue accounts for 1.6 wt% relative to the initial RLO and has an average Mw equal to 2728 g mol^{-1} (**Table S1**). The GPC profile (**Figure S13**) shows the presence of high-Mw species highly concentrated in the residue.

2. *^{1}H-^{13}C HSQC NMR and ^{31}P NMR*

To further evaluate the variability in molecular structures ^{1}H ^{13}C HSQC NMR was employed to assign and quantify the different end-units (EU) and inter-unit linkages (I-UL) across the six fractions (H100-E100) and the RLO.[92] The amount of end-units gradually decrease from H100 (83.6 %) > H80 (47.3%) > H60 (34%) > H40 (24.7%) > H20 (20.3%) > E100 (19.7%), as shown in **Figure S3**. The presence of end-units in the last fractions—i.e H40, H20, and E100—is due to the functional groups attached to the aromatic rings of the larger molecules, which are detectable with ^{13}C-^{1}H HSQC NMR. The amount of non-oxygenated end-units (i.e., Methyl, Ethyl, Propyl, and Propenyl) decreases over the fractions as follows: H100 (81.9%) > H80 (21.4%) > H60 (14.9%) > H40 (13.4%) > H20 (13%) > E100 (9.6%). The decreasing amount of non-oxygenated (apolar) end-units from H100 to E100 is attributed to the increasing polarity of the extraction solvent, due to the gradual addition of EtOAc to heptane. Furthermore, the number of oxygenated end-units (propanol and methoxy) changes as follow: H80 (25.9%) > H60 (19.1%) > H40 (11.2%) > E100 (10.1%) > H20 (7.2%) > H100 (1.7%). Herein, the proportion of oxygenated (polar) end-units increases across the six fractions as the polarity of the extraction solvent is gradually increased by the sequential addition of EtOAc to heptane.

Figure S4 illustrates the distribution of I-UL across the fractions, highlighting the structural differences in dimers, trimers, and larger oligomers within each fraction. In total 5 different oxygenated I-UL—β-5 γ-OH, β-1 γ-OH, β-β 2x γ-OH, β-β THF, and β-O-4 —and 5 different not-oxygenated I-UL—β–5 Ethyl, β–5 Propyl, β–1 Ethyl, β–1 Propyl, and 5-5 Biphenyl—were identified and quantified across the fractions (**Figure S4**), as result of the large variability in not-monomeric lignin-derived structures. The total amount of quantified I-UL increased progressively from H100 to E100, as follows: H100 (5.1%) < H80 (15.3%) < H60 (22.8%) < H40 (31.6%) < H20 (37%) < E100 (41.7%). This trend aligns with the GPC results, which supports the enrichment of high-molecular weight molecules from H100 to E100. The oxygenated I-UL increase across the fractions as follows: E100 (34.6%) > H20 (31%) > H40 (24.8%) > H60 (13.7%) > H80 (6%). Additionally, the not-oxygenated I-UL changes as follow: H80 (9.3%) > H60 (9.1%) > E100 (7.1%) > H40 (6.8%) > H20 (5.9%) > H100 (5.1%).

A comprehensive table containing all the EU and I-UL, along with their distribution across the fractions, is provided in **Tables S2** and **S3** of the ESI.

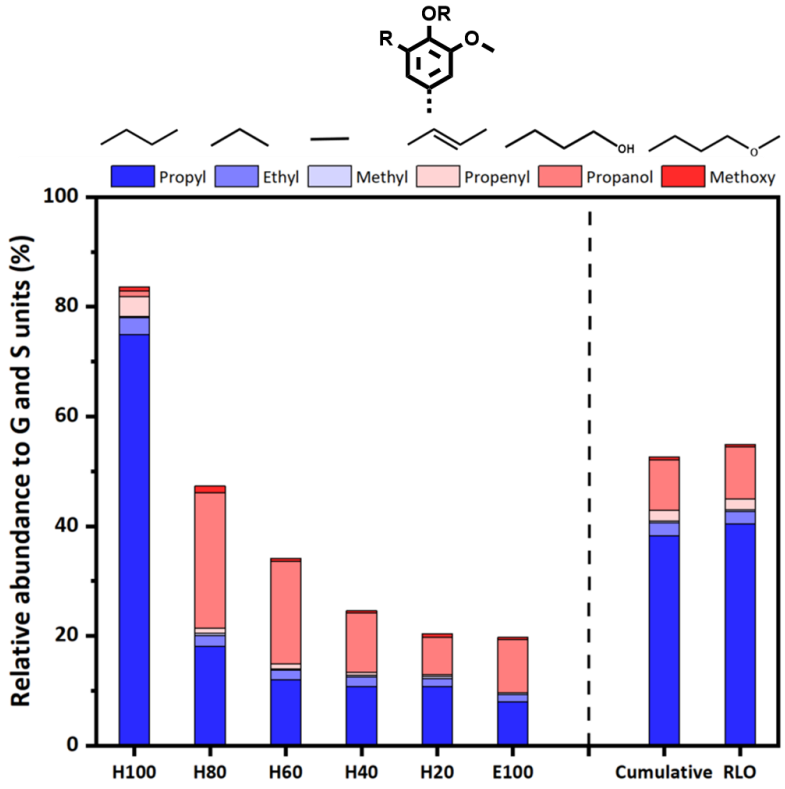

Figure S3. Relative abundance of end-units from 2D HSQC NMR for the obtained fractions (H100-E100).

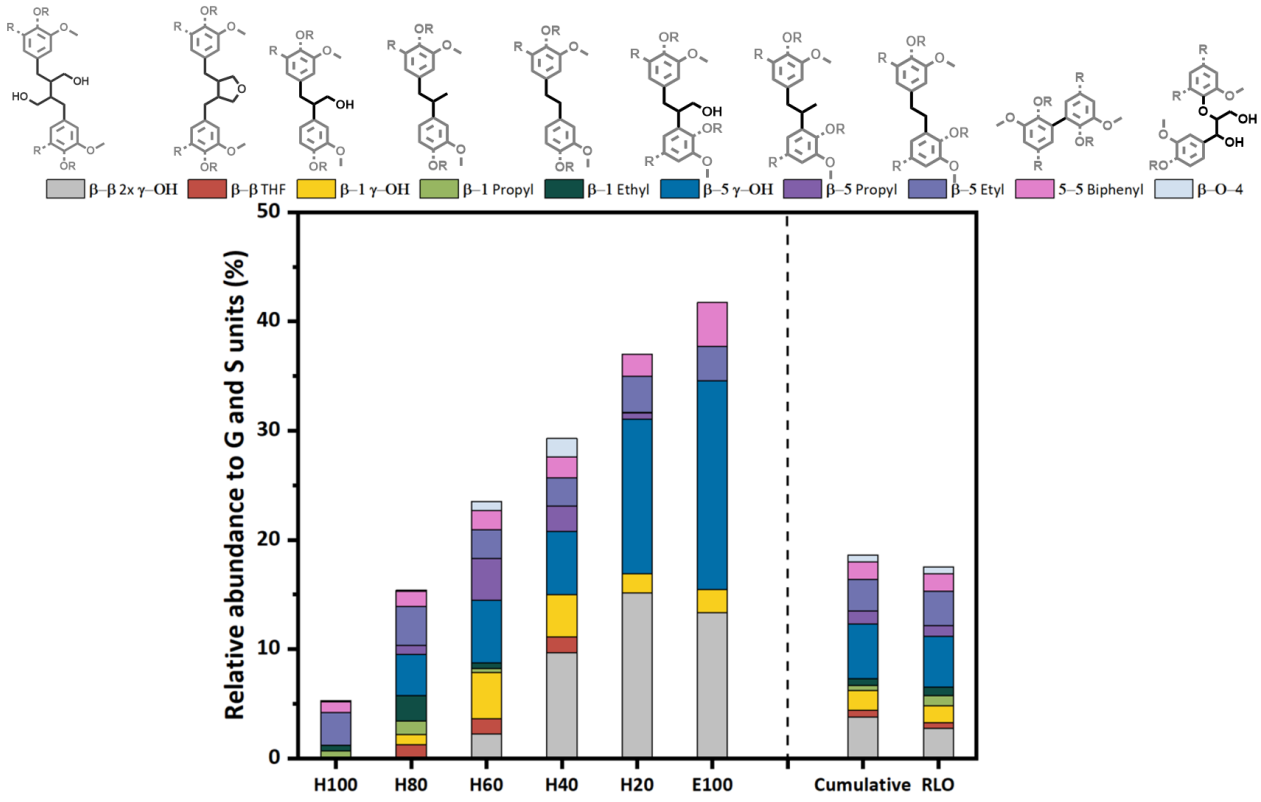

Figure S4. Relative abundance of inter-unit linkages from 2D HSQC NMR for the obtained fractions (H100-E100).

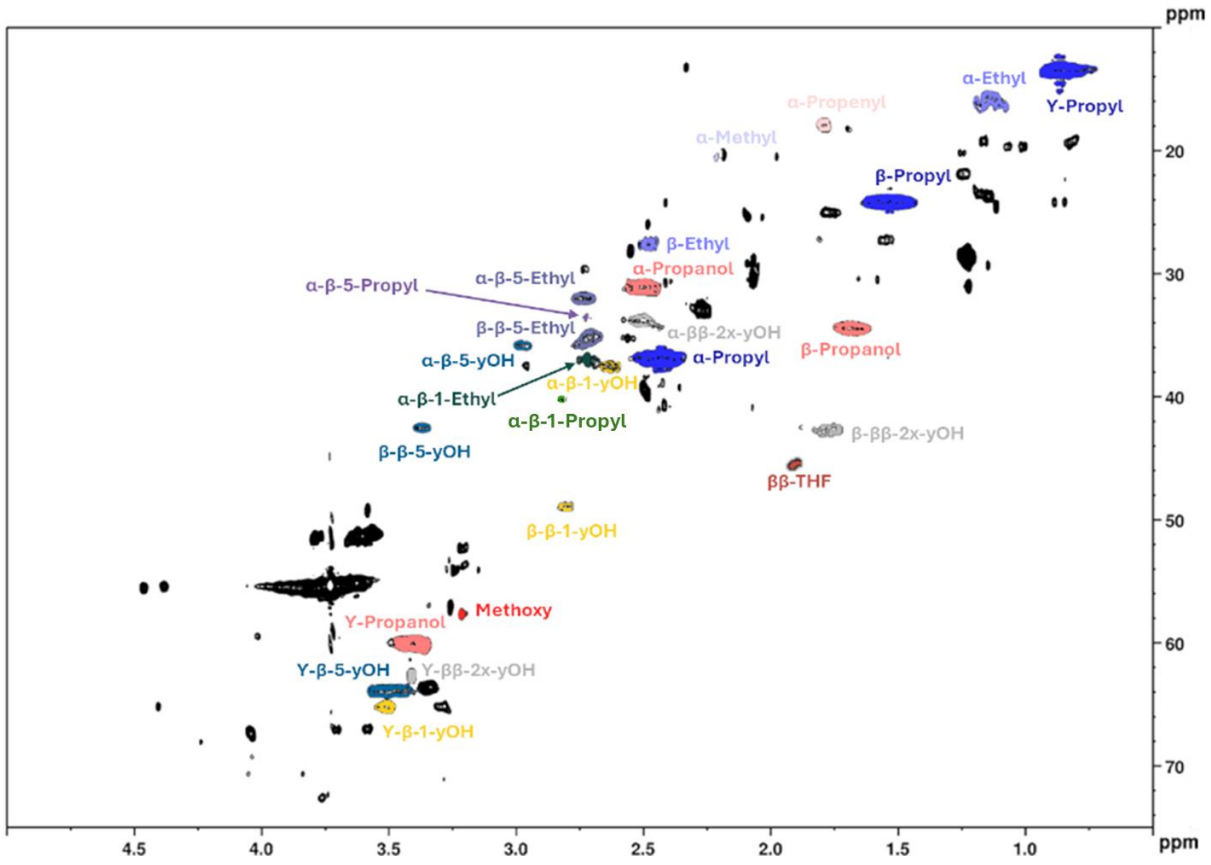

Scheme S2. Assigned $^{1}H–^{13}C$ HSQC NMR spectrum of the unfractionated RCF lignin oil. The annotated correlations correspond to the identified end-units (EU) and inter-unit linkages (I-UL). Colors used for signal assignment match those of the corresponding molecular structures shown in **Figures S3** and **S4**, facilitating cross-referencing between spectral features and structural motifs.

Table S2. Distribution of end-units from 2D HSQC NMR across the fractions and in the RLO.

EU	H100 (%)	H80 (%)	H60 (%)	H40 (%)	H20 (%)	E100 (%)	RLO (%)
Methyl	0.18	0.5	0.26	0.3	0.36	0.3	0.25
Ethyl	3	1.9	1.8	1.7	1.5	1.3	2.2
Propyl	74.9	18.1	12	10.8	10.7	8	40.4
Propenyl	3.7	0.89	0.87	0.6	0.4	0	2
Propanol	1.0	24.7	18.7	10.8	6.7	9.7	9.5
Methoxy	0.7	1.2	0.5	0.4	0.6	0.4	0.4
TOTAL	83.6	47.3	34	24.7	20.3	19.7	54.8

Table S3. Distribution of inter-unit linkage from 2D HSQC NMR across the fractions and in the RLO.

I-UL	H100 (%)	H80 (%)	H60 (%)	H40 (%)	H20 (%)	E100 (%)	RLO (%)
β-β 2x γ-OH	0	0	2.2	9.7	15.2	13.4	2.8
β-β THF	0	1.3	1.4	1.4	0	0	0.5
β-1 γ-OH	0	0.9	4.3	4.3	1.7	2.1	1.5
β-1 Ethyl	0.4	2.3	0.5	0	0	0	0.6
β-1 Propyl	0.7	1.2	0.4	0	0	0	0
β-5 γ-OH	0	3.8	5.8	9.4	14.2	19.1	3.6

β-5 Ethyl	3	3.6	2.6	2.6	3.3	3.1	3.2
β-5 Propyl	0	0.8	3.8	2.3	0.6	0	1
5-5 Biphenyl	1	1.4	1.8	1.9	2	4	1.6
β-O-4	0.1	0	0.8	1.7	0	0	0
TOTAL	5.2	15.3	23.6	33.3	37	41.7	14.8

Moreover, **Figure S5** reports the hydroxyl group content (mmol g^{-1}) across the fractions as determined by ^{31}P NMR and provides additional insight into the polarity evolution induced by the fractionation protocol. As the fractionation is carried out via sequential solvent extraction using solvent mixtures of progressively increasing polarity, the observed hydroxyl group trends directly reflect variations in fraction polarity. In particular, the aliphatic OH content increases monotonically from H100 to E100, indicating a progressive enrichment of oxygenated functionalities in the heavier fractions. This observation is fully consistent with the $^{1}H–^{13}C$ HSQC NMR results, which showed an increasing contribution of oxygenated inter-unit linkages (I-UL) from H100 to E100. The combined HSQC and ^{31}P NMR analyses therefore confirm that the heavier fractions are not only richer in high-molecular-weight species, but also more strongly oxygenated, with oxygen functionality predominantly associated with inter-unit linkages rather than end-units. In contrast, the phenolic OH content decreases from H100 to E100 when expressed on a mass basis, reflecting the higher abundance of monomeric, chain-end-rich species in the lighter fractions and the dilution of phenolic end groups in increasingly oligomeric material. Overall, the ^{31}P NMR data reveal clear polarity trends across the fractions and provide complementary information that helps rationalize the fractionation behavior, while offering a basis for further discussion of structure–property relationships in lignin oil fractionation.

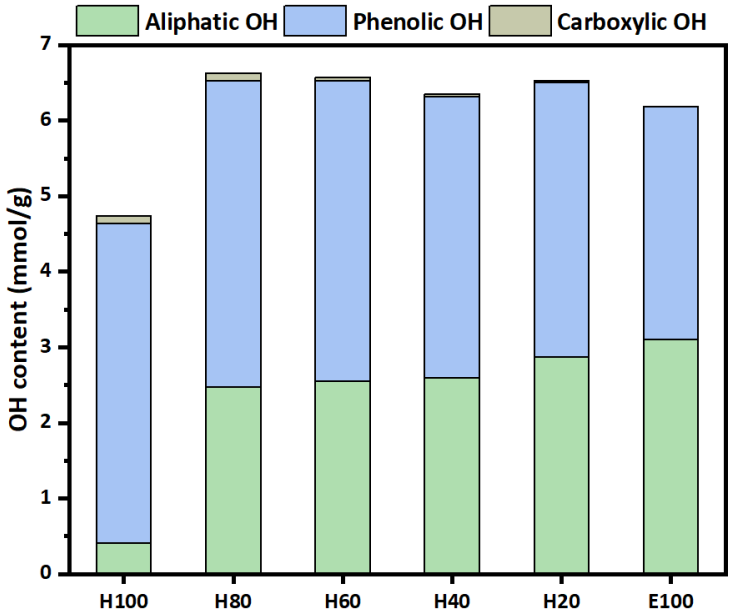

Figure S5. Hydroxyl group content of all fractions quantified by 31P-NMR and expressed as mmol g^{-1}.

C. ADDITIONAL INFORMATION

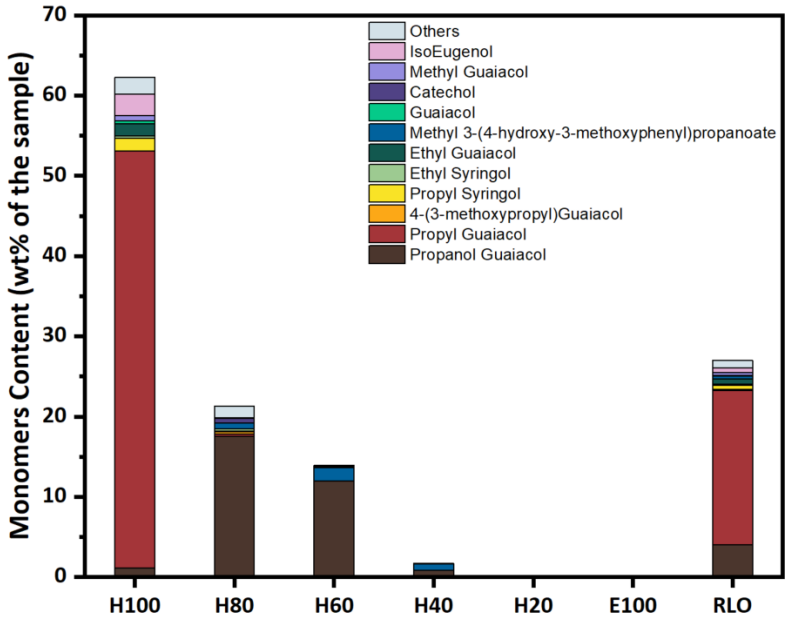

Figure S6. Monomer content for the obtained fractions (H100-E100) and RLO from GCxGC-FID.

Table S4. Distribution of all identified monomers across the fractions and in the RLO.

	H100 (wt%)	H80 (wt%)	H60 (wt%)	H40 (wt%)	H20 (wt%)	E100 (wt%)	RLO (wt%)
M1	1.58	0.10	0	0	0	0	0.51
M2	51.90	0.29	0	0	0	0	19.23
M3	0.76	0.28	0	0	0	0	0.37
M4	0	0	0	0	0	0	0
M5	1.12	17.60	11.98	0.82	0.03	0.04	3.99
M6	0	0.22	0.12	0.04	0	0	0.07
M7	0.29	0.31	0	0	0	0	0.16
M8	1.51	0	0	0	0	0	0.63
M9	0	0.58	0.16	0	0	0	0.11
M10	0.14	0	0	0	0	0	0.06
M11	2.68	0.07	0	0	0	0	0.60
M12	0.03	0	0	0	0	0	0
M13	0.69	0.04	0	0	0	0	0.33
M14	0	0.24	0	0	0	0	0.16
M15	0.34	0	0	0	0	0	0
M16	0	0.70	1.66	0.83	0.07	0.01	0.35
M17	0.80	0.59	0	0	0	0	0.41
M18	0.04	0.27	0	0	0	0	0
TOTAL	62.30	21.30	13.91	1.69	0.10	0.05	26.99

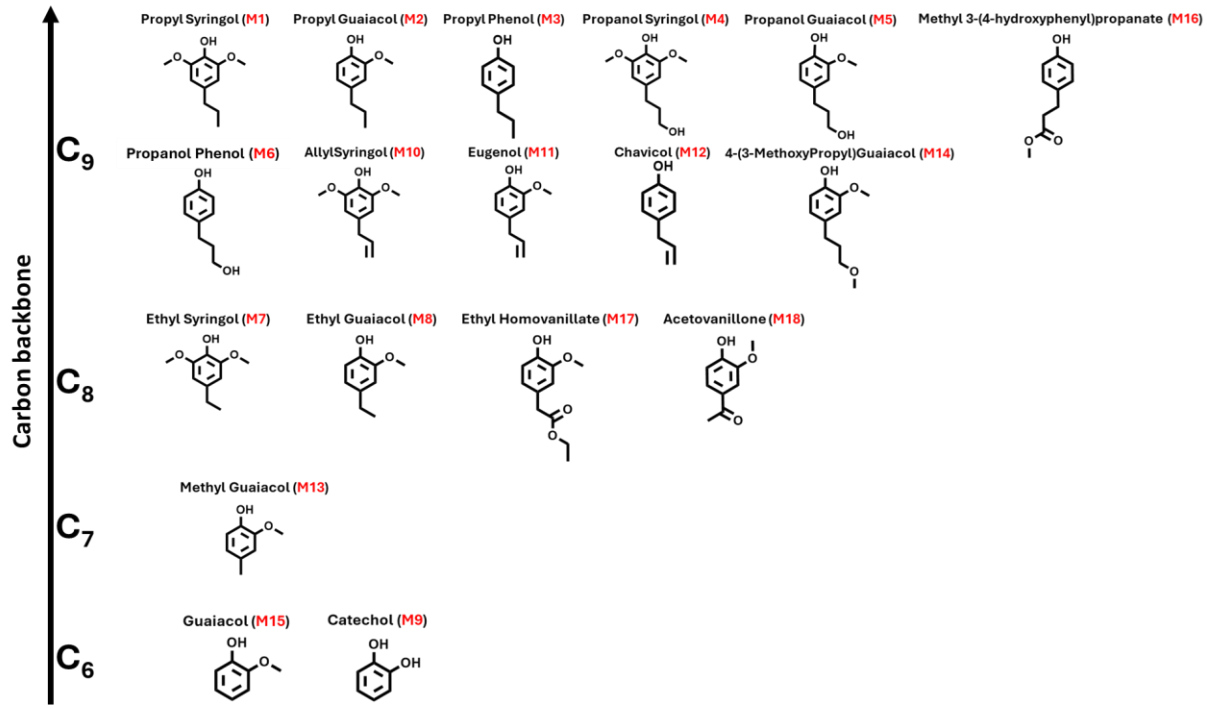

Scheme S3. All identified monomers across the six fractions (H100-E100) and RLO with GCxGC-MS as a function of the carbon backbone.

Table S5. Distribution of β-5 dimers (in wt%) across the fractions and in the RLO.

β-5	R_1	H100	H80	H60	H40	H20	E100	RLO
1	$(CH_2)_2CH_2OH$	0.0	0.5	1.7	0.7	0.0	0.0	0.4
2	$(CH_2)_2CH_3$	4.3	2.4	0.0	0.0	0.0	0.0	1.9
3	CH_2CH_3	0.2	0.1	0.0	0.0	0.0	0.0	0.0
4	H	0.0	0.1	0.0	0.0	0.0	0.0	0.0
5	$(CH_2)_2CHOCH_3$	0.0	0.0	0.0	0.0	0.0	0.0	0.0
6	//	0.0	0.0	0.0	0.0	0.0	0.0	0.0
7	//	0.0	1.2	0.0	0.0	0.0	0.0	0.0
8	//	0.0	0.1	0.0	0.0	0.0	0.0	0.0
TOTAL		4.5	4.4	1.7	0.7	0.0	0.0	2.3

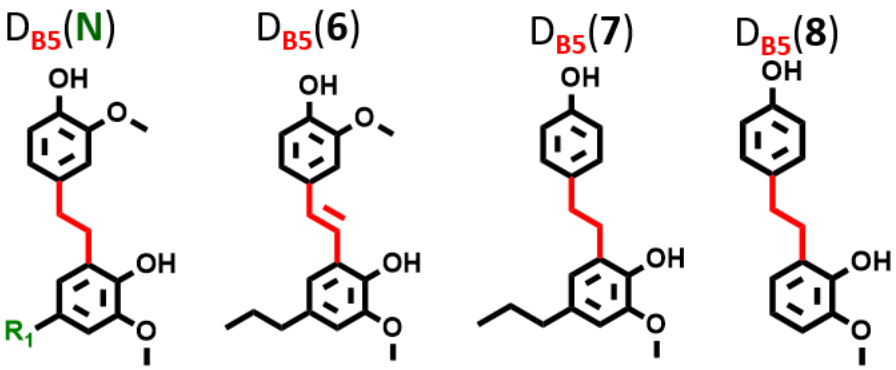

Table S6. Distribution of β-5 P dimers (in wt%) across the fractions and in the RLO.

β-5 P	R_1	H100	H80	H60	H40	H20	E100	RLO
1	$(CH_2)_2CH_2OH$	0.0	0.8	1.3	0.8	0.0	0.0	0.5
2	$(CH_2)_2CH_3$	0.7	0.0	0.0	0.0	0.0	0.0	0.4
3	CH_2CH_3	0.1	0.0	0.0	0.0	0.0	0.0	0.0
4	$(CH_2)_2CHOCH_3$	0.0	0.7	4.2	1.8	0.0	0.0	0.9
5	$(CH_2)_2CHOH$	0.0	0.0	1.0	0.8	0.0	0.0	0.2
TOTAL		0.8	1.6	6.5	3.4	0.0	0.0	2.0

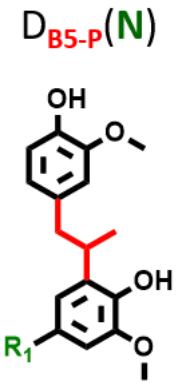

Table S7. Distribution of β-5 γ-OH dimers (in wt%) across the fractions and in the RLO.

β-5 γ-OH	R_1	H100	H80	H60	H40	H20	E100	RLO
1	$(CH_2)_2CH_2OH$	0.0	0.0	1.5	3.1	1.1	0.1	0.7
2	$(CH_2)_2CH_3$	0.2	5.7	6.3	0.3	0.0	0.0	1.6
3	CH_2CH_3	0.0	0.0	0.3	0.0	0.0	0.0	0.1
TOTAL		0.2	5.7	8.3	3.4	1.1	0.1	2.4

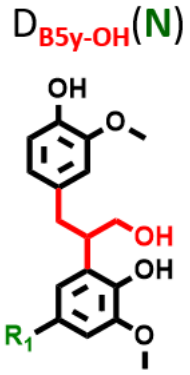

Table S8. Distribution of 5-5 dimers (in wt%) across the fractions and in the RLO.

5-5	R_1	R_2	H100	H80	H60	H40	H20	E100	RLO
1	$(CH_2)_2CH_2OH$	$(CH_2)_2CH_2OH$	0.0	0.0	0.0	0.0	0.4	0.1	0.2
2	$(CH_2)_2CH_2OH$	$(CH_2)_2CH_3$	0.0	0.9	2.2	0.4	0.0	0.0	0.4

3	$(CH_2)_2CH_2OH$	CH_2CH_3	0.0	0.0	0.0	0.0	0.0	0.0	0.0
4	$(CH_2)_2CH_3$	$(CH_2)_2CH_3$	2.0	0.8	0.0	0.0	0.0	0.0	1.0
5	$(CH_2)_2CH_3$	CH_2CH_3	0.4	0.2	0.0	0.0	0.0	0.0	0.2
6	CH_2CH_3	CH_2CH_3	0.2	0.4	0.0	0.0	0.0	0.0	0.1
7	CH_2CH_3	CH_3	0.1	0.2	0.0	0.0	0.0	0.0	0.0
8	$(CH_2)_2CH_3$	CH_3	0.0	0.0	0.0	0.0	0.0	0.0	0.0
9	$(CH_2)_2CH_3$	$(CH_2)_2CH_2OCH_3$	0.0	0.4	0.0	0.0	0.9	0.0	0.1
10	$(CH_2)_2CH_2OH$	$(CH_2)_2CHOH$	0.0	0.0	0.3	1.2	0.0	0.2	0.3
11	CH_2CH_3	$(CH_2)_2CH_2OCH_3$	0.0	0.7	0.5	0.0	0.0	0.0	0.1
12	$(CH_2)_2CH_2OCH_3$	CH_2CHCH_3	0.0	0.1	0.9	0.0	0.0	0.0	0.0
TOTAL			2.7	3.7	3.9	1.6	1.3	0.3	2.4

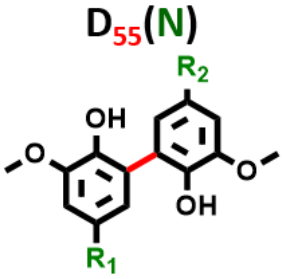

Table S9. Distribution of others (β-O-4) dimers (in wt%) across the fractions and in the RLO.

β-O-4	R_1	H100	H80	H60	H40	H20	E100	RLO
1	$(CH_2)_2CH_3$	0.0	0.0	0.0	0.0	0.0	0.0	0.0
2	$(CH_2)_2CHOCH_3$	0.0	1.2	0.5	0.0	0.0	0.0	0.2
3	$(CH_2)_2CH_2OH$	0.0	0.0	0.6	0.8	0.1	0.0	0.2
4	$(CH_2)_2CH_2OCH_3$	0.0	0.0	0.2	0.0	0.0	0.0	0.0
5	$(CH_2)_2CH_3$	0.0	0.0	0.0	0.0	0.0	0.0	0.0
TOTAL		0.0	1.2	1.3	0.8	0.1	0.0	0.4

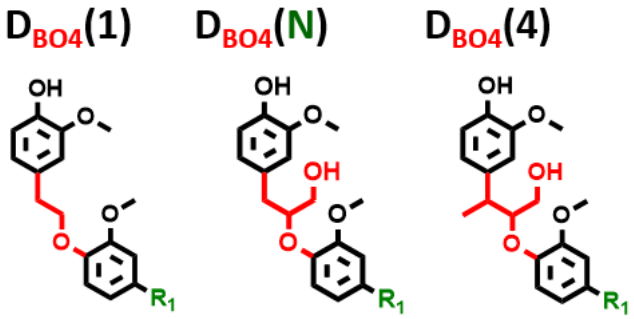

Table S10. Distribution of others (4-O-5) dimers (in wt%) across the fractions and in the RLO.

4-O-5	R_1	R_2	H100	H80	H60	H40	H20	E100	RLO
1	CH_2CH_3	$(CH_2)_2CHOCH_3$	1.5	0.2	0.0	0.0	0.0	0.0	0.6
2	$(CH_2)2CH_2OCH_3$	$(CH_2)_2CHOCH_3$	0.0	0.0	0.0	0.0	0.0	0.0	0.0
3	$(CH_2)_2CH_2OH$	$(CH_2)_2CH_2OH$	0.0	0.0	0.0	0.0	0.0	0.0	0.0
TOTAL			1.5	0.2	0.0	0.0	0.0	0.0	0.6

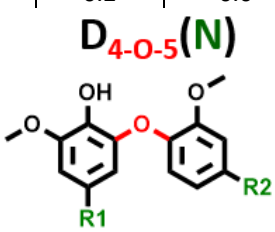

Table S11. Distribution of β-1 dimers (in wt%) across the fractions and in the RLO.

β-1	R_1	H100	H80	H60	H40	H20	E100	RLO
1	//	0.4	1.5	0.1	0.0	0.0	0.0	0.3
2	//	0.6	3.3	0.5	0.0	0.0	0.0	0.6
3	//	0.0	1.6	7.1	3.3	0.2	0.0	1.7
TOTAL		1.0	6.4	7.7	3.3	0.2	0.0	2.6

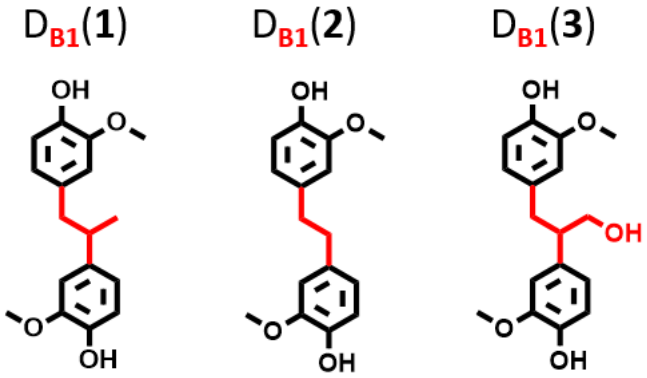

Table S12. Distribution of β-β dimers (in wt%) across the fractions and in the RLO.

β-β	R_1	H100	H80	H60	H40	H20	E100	RLO
1	//	0.0	0.0	1.6	3.7	1.4	0.0	0.7
2	//	0.0	0.8	0.8	0.0	0.0	0.0	0.2
3	//	0.0	0.9	0.0	0.0	0.0	0.0	0.1
TOTAL		0.0	1.7	2.4	3.7	1.4	0.0	1.0

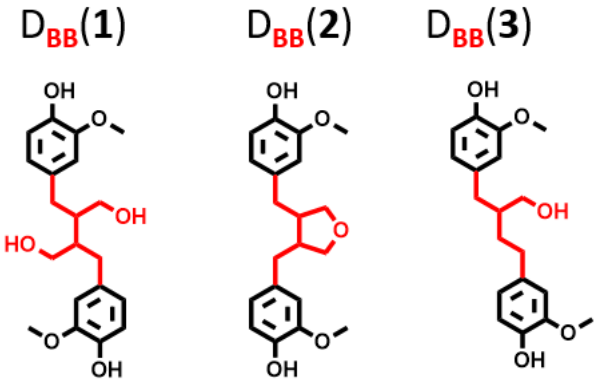

Table S13. Distribution of others (phenyl-coumaran) dimers (in wt%) across the fractions and in the RLO.

Unsorted	R_1	H100	H80	H60	H40	H20	E100	RLO
1	//	0.3	1.9	0.4	0.0	0.0	0.0	0.4
2	//	0.3	0.6	0.0	0.0	0.0	0.0	0.2
3	//	0.3	0.1	0.0	0.0	0.0	0.0	0.1
TOTAL		0.9	2.6	0.4	0.0	0.0	0.0	0.7

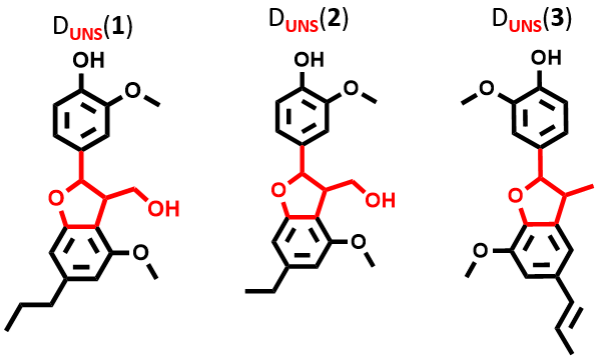

Table S14. List of all the hydrocarbons identified in the liquid products divided by their carbon number. The table includes all the hydrocarbons that have been identified through GC-MS and included in the products from HDO of the different fractions.

ENTRY	RT (min)	C_n	NAME	STRUCTURE
MONOMER-DERIVED (C_6-C_{11})				
1	2.913	6	Methyl-cyclopentane	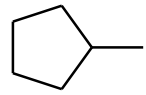
2	3.233	6	Cyclohexane	
3	3.502 and 3.546	7	Dimethyl-cyclopentane	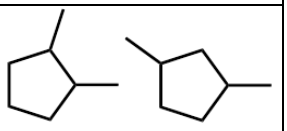
4	3.969	7	Methyl-cyclohexane	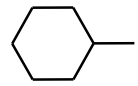
5	4.120	7	Ethyl-cyclopentane	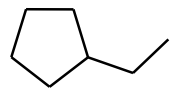
6	4.799	8	1,2-dimethyl-cyclohexane	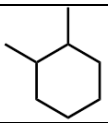
7	4.968	8	1-ethyl-2-methyl-cyclopentane	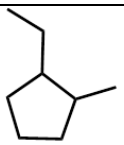
8	5.689	8	Propyl-cyclopentane	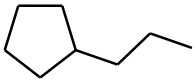
9	5.710	8	Ethyl-cyclohexane	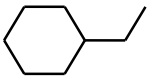

10	6.683	9	1-methyl-2-propyl- cyclopentane	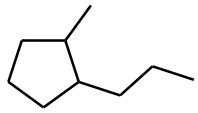
11	7.041	9	1-mehtyl-2-ethyl- cyclohexane	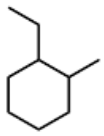
12	7.283	9	Methylethyl- cyclohexane	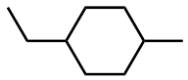
13	7.443	9	Propyl-cyclohexane	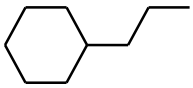
14	8.414	10	1-methyl-2-propyl- cyclohexane	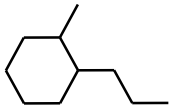
15	9.188	10	1-methylpropyl-cyclohexane	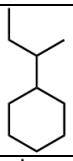
16	9.289	10	2-methylpropyl-cyclohexane	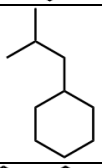
17	10.758	11	2-methyl-decahydronaphthalene	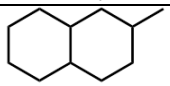
DIMER-DERIVED (C_{12}-C_{18})				
18	13.947	12	5,5-bicyclohexyl	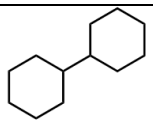
19	14.320	13	Heptyl-cyclohexane (?)	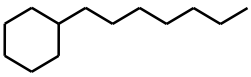
20	14.929	13	2-methyl-1,1'- bicyclohexane	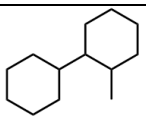
21	16.192	14	2-ethyl-1,1'- bicyclohexane	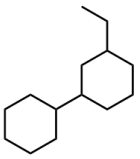
22	16.519	14	1,2-dicyclohexylethane	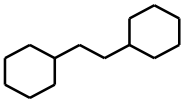

23	17.416	15	Propane-1,2- diyldicyclohexane	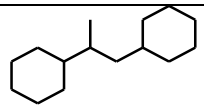
24	17.950	16	1,4-dicyclohexylbutane	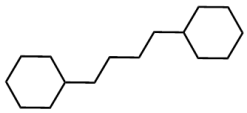
25	18.687	16	1-(2-cyclohexylethyl)- 3-ethylcyclohexane	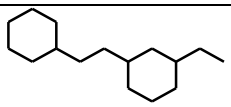
26	19.452	17	3-ethyl-3'-propyl-1,1'-bi(cyclohexane)	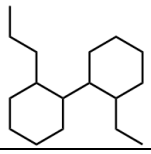
27	19.887	17	1-(2-cyclohexylethyl)-3-propylcyclohexane	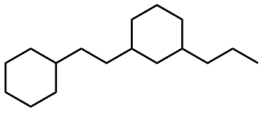
28	20.083	17	1-(1-cyclohexylpropan-2-yl)-3-ethylcyclohexane	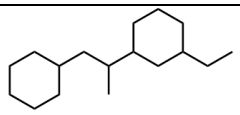
29	20.696	18	1-(1-cyclohexylpropan-2-yl)-3-propylcyclohexane	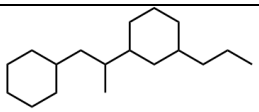
30	20.784	18	3,3'-dipropyl-1,1'-bi(cyclohexane)	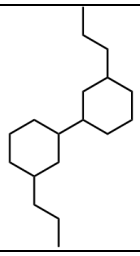

Table S15. Carbon-based relative carbon yield (RCY) for different catalysts.

C number	Ni/SiO2	Ru/C	Pd/C	Ni2P/SiO2 spent	Ni2P/SiO2
Relative Carbon Yield (%)					
6	1.49	1.78	0.79	1.19	2.22
7	2.55	9.99	1.00	1.88	1.53
8	9.03	12.80	2.89	6.55	7.52
9	22.35	14.22	5.60	22.95	24.43
10	2.95	6.88	1.22	2.95	4.30
11	6.93	4.018	4.93	3.97	3.69
12	0.28	0.26	0.17	0.096	0.51
13	1.17	0.85	0.58	0.65	1.09
14	2.93	1.34	0.89	3	3.7
15	1.42	0.90	0.42	1.86	2.28

16	2.26	0.33	0.87	2.02	2.36
17	7.097	0.62	3.30	5.7	7.73
18	1.89	0.11	0.89	1.9	2.16
19	1.95	0.86	2.45	2.4	2.28
20	0.10	0.048	0.13	0.13	0.12
21	0.29	0.13	0.38	0.37	0.32
22	0.65	0.30	0.85	0.83	0.67
23	0.85	0.40	1.10	1.078	0.91
24	0.51	0.23	0.66	0.64	0.52
25	1.02	0.48	1.32	1.29	1.00
26	1.52	0.71	1.97	1.93	1.44
27	0	0	0	0	0
Oxygenates	0	0	11.2	0	0
TOTAL	**69.3**	**57.4**	**43.7**	**63.5**	**71**
C6-C11	45.3	49.7	16.5	39.5	43.7
C12-C18	17	4.5	7.1	15.3	19.9
C19-C27	7	3.2	8.9	8.7	7.4

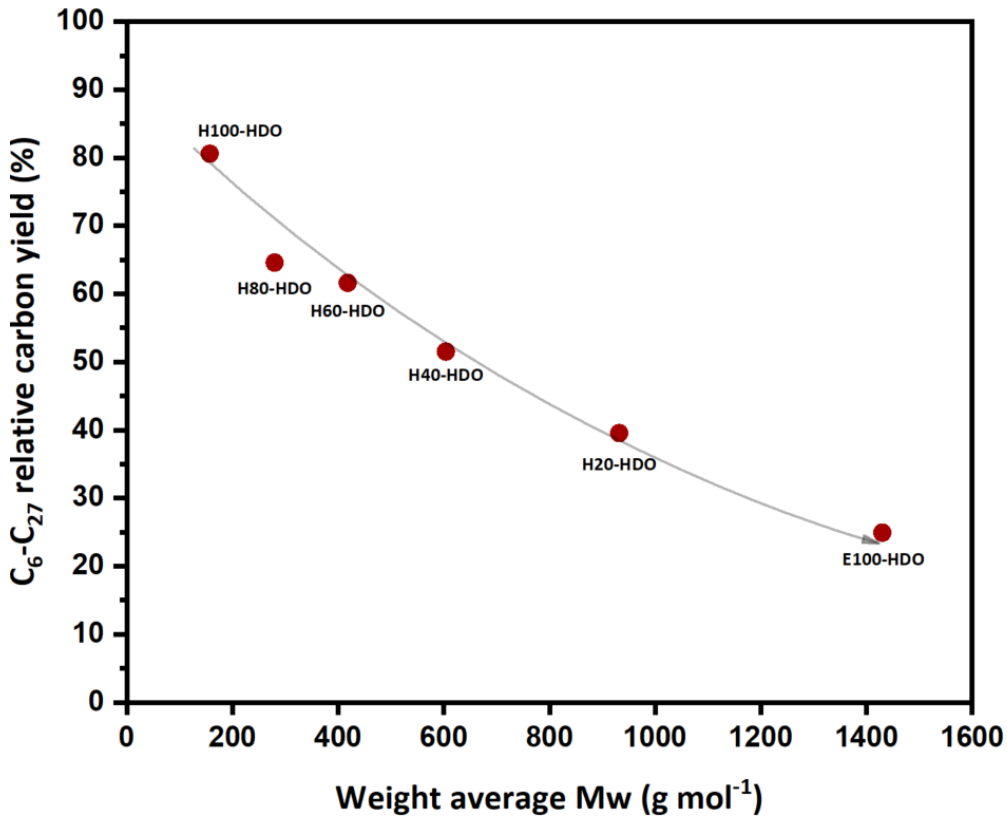

Figure S7. Relative carbon yield (C_6-C_{27}) as function of the weight average molecular weight for the six fractions (H100-E100).

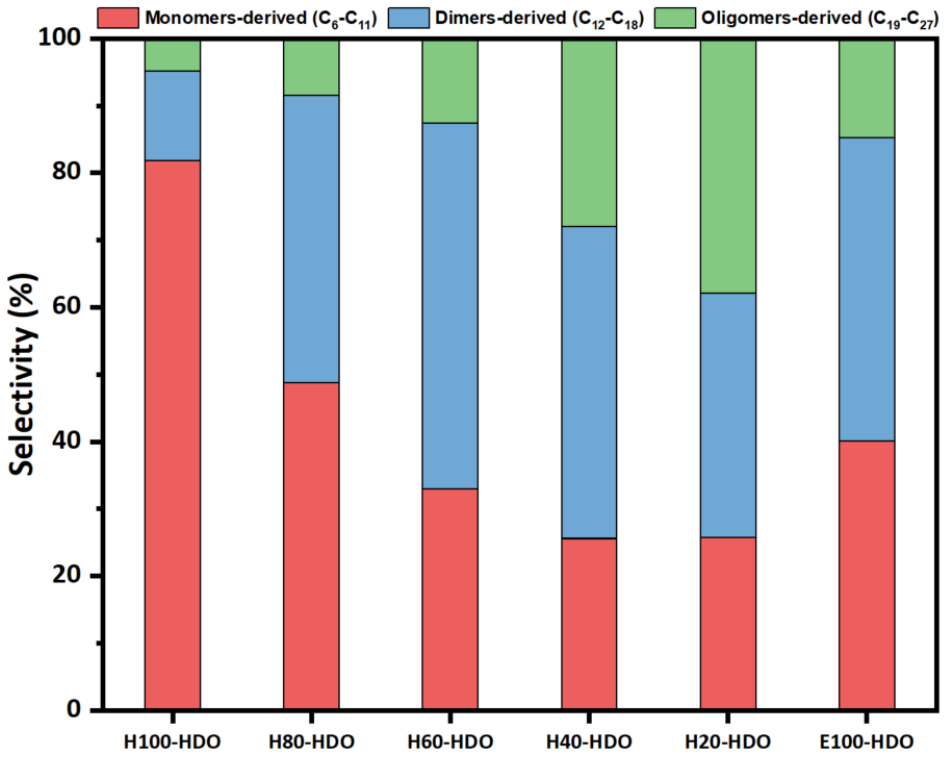

Figure S8. Selectivity of the different class of hydrocarbons for the HDO products from different fractions (H100-HDO-E100-HDO).

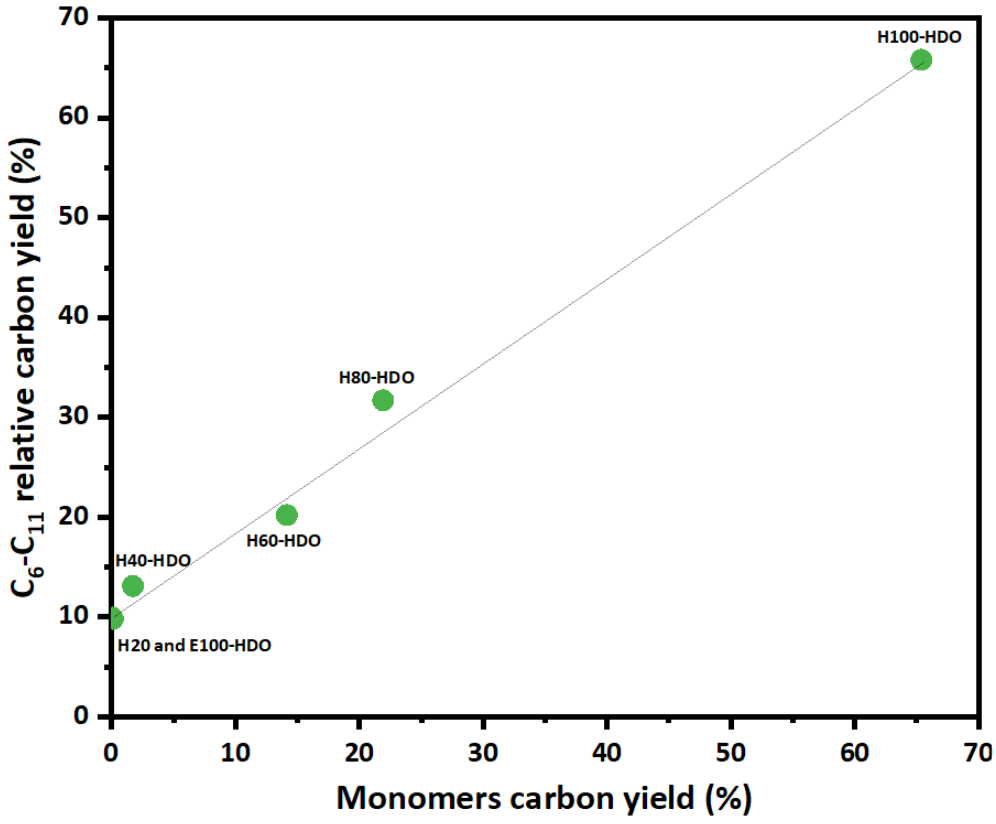

Figure S9. Relative carbon yield of C_6-C_{11} hydrocarbons as function of the monomer carbon yield for the different fractions (H100-E100).

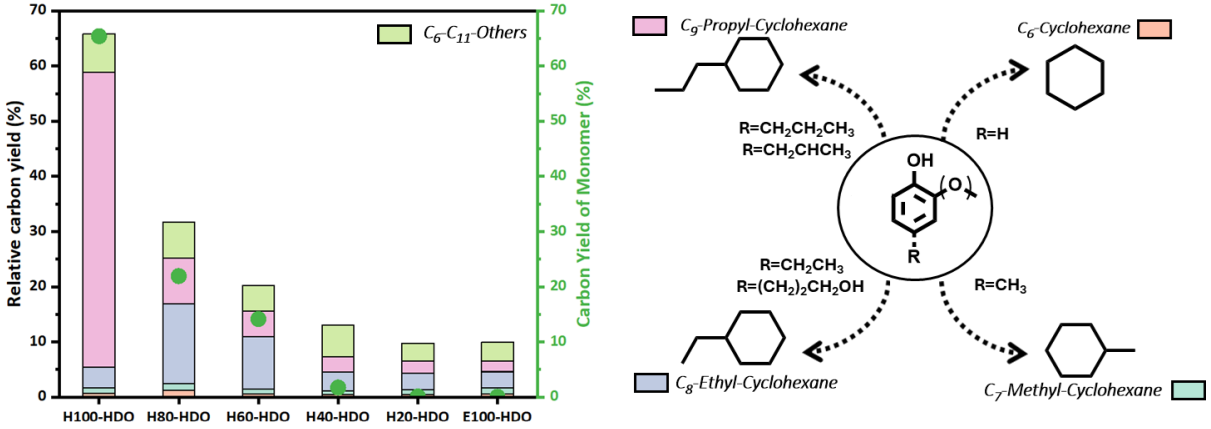

Figure S10. (left) Relative carbon yield of C_9-propyl-cyclohexane, C_8-ethyl-cyclohexane, C_7-methyl-cyclohexane, C_6-cyclohexane and others C_6-C_{11} hydrocarbons for the HDO products of the six different fractions (H100-HDO-E100-HDO), and (right) proposed major conversion pathways of lignin-derived monomers.

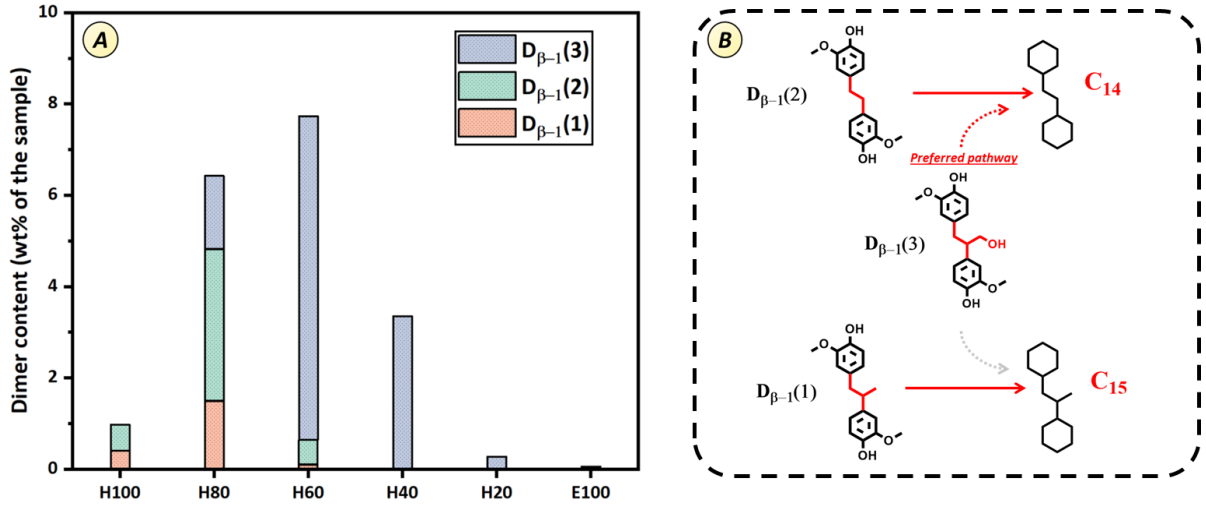

Figure S11. a) β-1 dimers content identified and quantified via GCxGC-MS/FID for the obtained fractions (H100-E100), **b)** Proposed major conversion pathways to C_{14}-C_{15} dimers-derived hydrocarbons from β-1 dimers

References:

1 K. Van Aelst, E. Van Sinay, T. Vangeel, E. Cooreman, G. Van Den Bossche, T. Renders, J. Van Aelst, S. Van Den Bosch and B. F. Sels. (2020). Reductive catalytic fractionation of pine wood: Elucidating and quantifying the molecular structures in the lignin oil. *Chem. Sci.*, **11**, 11498–11508.

2 H. Dao Thi, K. Van Aelst, S. Van den Bosch, R. Katahira, G. T. Beckham, B. F. Sels and K. M. Van Geem. (2022). Identification and quantification of lignin monomers and oligomers from reductive catalytic fractionation of pine wood with GC × GC – FID/MS. *Green Chem.*, **24**, 191–206.

3 J. T. Scanlon and D. E. Willis. (1985). Calculation of flame ionization detector relative response factors using the effective carbon number concept. *J. Chromatogr. Sci.*, **23**, 333–340.

4 Z. Cao, M. Dierks, M. T. Clough, I. B. Daltro de Castro and R. Rinaldi. A Convergent Approach for a Deep

Converting Lignin-First Biorefinery Rendering High-Energy-Density Drop-in Fuels. *Joule*, **2**, 1118–1133.